Measurement of the distribution of bond angles in H_2O^+

D. Zajfman and A. BelkacemT. GraberE. P. Kanter and R. E. MitchellR. NaamanZ. VagerB. J. Zabransky

Citation: The Journal of Chemical Physics **94**, 2543 (1991); doi: 10.1063/1.459881
View online: http://dx.doi.org/10.1063/1.459881
View Table of Contents: http://aip.scitation.org/toc/jcp/94/4
Published by the American Institute of Physics

Measurement of the distribution of bond angles in H_2O^+

D. Zajfman and A. Belkacem[a)]
Physics Division, Argonne National Laboratory, Argonne, Illinois 60439

T. Graber
Physics Division, Argonne National Laboratory, Argonne, Illinois 60439 and Department of Physics, University of Illinois at Chicago, Chicago, Illinois 60680

E. P. Kanter and R. E. Mitchell[b)]
Physics Division, Argonne National Laboratory, Argonne, Illinois 60439

R. Naaman
Department of Chemical Physics, Weizmann Institute, Rehovot, Israel

Z. Vager
Physics Division, Argonne National Laboratory, Argonne, Illinois 60439 and Department of Nuclear Physics, Weizmann Institute, Rehovot, Israel

B. J. Zabransky
Physics Division, Argonne National Laboratory, Argonne, Illinois 60439

(Received 1 November 1990; accepted 7 November 1990)

A quantitative analysis of the bending mode of H_2O^+ is made using the Coulomb Explosion technique. The full extent of the angular distribution is measured and is in good agreement with the previously measured bending frequency. The equilibrium value for the angle is extracted from the data with high precision and is in excellent agreement with theoretical predictions as well as spectroscopic measurements.

I. INTRODUCTION

The water cation (H_2O^+) is an open-shell cation of considerable interest. Over the years, there have been extensive photoelectron spectroscopy studies of H_2O^+[1-3] that have determined the ionization potential and frequencies of the symmetric stretching (ν_1) and bending (ν_2) modes. Direct optical spectroscopy was first done by Lew and Heber[4,5] who observed the $\tilde{A}^2A_1 - \tilde{X}^2B_1$ transitions. H_2O^+ was also detected in comet Kohoutek by Herzberg and Lew[6] and by Wehinger *et al.*[7] Recently, Dinelli, Crofton, and Oka[8] have measured the frequency of the ν_3 (antisymmetric stretching) infrared band. The ground state structure, which has been well established by spectroscopic methods, has also been reported by several groups.[5,8,9] H_2O^+ has also been the subject of *ab initio* calculations by Smith *et al.*,[10] Fortune *et al.*,[11] and Esposti *et al.*[12] among others.

In this paper, we report our direct observation of the structure, and bending mode vibrations, of H_2O^+ using the Coulomb Explosion Imaging (CEI) technique. In order to establish this technique as a quantitative source of information on molecular structures, it is important to study systems with structures that have been experimentally determined by other methods. H_2O^+ is ideal for this purpose. (The existing experimental and theoretical results are summarized in Table I.) We demonstrate that this method is able to determine the density distribution of the H-O-H angles and extract precise values of θ_e from the measured distribution. The observed bending frequency and angle are consistent with previous experimental and theoretical results.

II. EXPERIMENTAL DETAILS

Coulomb Explosion Imaging is a technique that provides direct information on the nuclear densities within a molecule by imaging individual molecules. The method, which has been described in detail elsewhere,[13] involves the foil-induced dissociation of a fast (MeV) beam of molecules. Through their mutual Coulomb repulsion, the resulting charged atomic ions convert their Coulomb energy into kinetic energy of relative motion. For a molecule containing N atoms, measurements of the $3N$ velocity components after the explosion provides information on the $3N$ spatial components within the original molecule. Since the time scale for electron stripping in the foil is very short compared to the characteristic vibrational and rotational motions in the molecule, the Coulomb explosion of each individual molecular ion gives a "snapshot" of the relative positions of the nuclei within that molecule. Combining such measurements for a large ensemble of molecules yields the fully correlated many-particle density distribution describing the nuclear coordinates of that ensemble.

In the experiment reported here, the molecular ions were formed by 40 eV electron bombardment of water vapor, at a pressure of ~ 10 mTorr. After extraction from the source, the ions were accelerated by the Argonne 4.5 MV Dynamitron accelerator to an energy of 4.230 MeV, magnetically mass analyzed, and then dissociated in a thin

[a)]Present address: Lawrence Berkeley Laboratory, Berkeley, CA, 94720.
[b)]Present address: Department of Chemistry, Univ. of Minnesota, Minneapolis, Minnesota 55455.

 0021-9606/91/042543-05$002.10

TABLE I. Experimental and theoretical results for the geometry and frequencies of H_2O^+.

	r_0 (Å)	r_e (Å)	θ_0 (deg)	θ_e (deg)	ν_1 (cm^{-1})	ν_2 (cm^{-1})	ν_3 (cm^{-1})
				Theories			
Ref. 10	···	0.9816	···	112.4	3887	1582	3979
Ref. 11	···	1.00738	···	108.5	3388	1518	3469
Ref. 12	···	0.997	···	109.1	···	···	···
				Experiments			
Ref. 1	···	···	···	···	3200(50)	1380(50)	···
Ref. 2	···	···	···	···	3220(40)	1370(40)	···
Ref. 3	1.03	···	109.4	···	···	···	···
Ref. 5	0.9988	···	110.46	···	···	1408	···
Ref. 8	0.989(8)	1.001	111.0(18)	108.9	3213.00(9)	···	3259.031(3)
Ref. 9	1.006(7)	···	109.8(16)	···	···	···	···
This work	···	1.00(4)	···	108.4(5)	···	1370(100)	···

(~100 Å) Formvar film. The resulting fragment ions were charge-state analyzed by an electrostatic deflector and, after a path of ~6 m, were detected in triple coincidence by the SAM-MUPPATS detector system.[14,15] The deflections were adjusted so that the oxygen fragments struck the SAM detector and the protons were recorded by the MUPPATS detector. For each molecule, this system records the x and y coordinates (transverse to the beam direction), as well as the relative time of arrival of each fragment ion. From this information, the three components of the velocity (relative to the center of mass) of each fragment are deduced.

III. DATA ANALYSIS

The set of $3N$ (nine in the H_2O^+ case) measured velocities is called an "event." For each event, the three translational velocities of the center of mass (CM), the three rotational angles, and the $3N$-6 (three in this case) structural body velocities are calculated. We call these velocities the "V-space" coordinates. The latter three contain all the structural information for this triatomic molecule. We choose for those coordinates the magnitudes of the two relative velocities between the oxygen and each proton ($|\mathbf{v}_a|$ and $|\mathbf{v}_b|$) and the angle between those two velocity vectors (θ_v). These V-space coordinates can, in principle, be directly related to the corresponding "R-space" coordinates describing the fully-correlated spatial geometry of the nuclei for each individual event.

The accuracy with which this transformation can be done depends on the experimental resolution of the detectors as well as on smearing effects due to the various collisional phenomena that affect the fragment ion trajectories during passage through the foil.[16] These effects can, for stiff vibrations, mimic the vibrational motions and thus must be deconvoluted from the measured distributions. At the relatively low beam-energies employed here, the most important of these effects is the small-angle multiple scattering of the fragment ions by the atoms of the target.[17] In order to take account of this effect, the transformation from V- to R-space coordinates is done by carrying out computer simulations of the experiment. The simulations, which have been described in detail elsewhere,[17] reproduce the smearing effect due to the interaction with the foil and, for a given initial R-space geometry, produce a set of events comparable to those measured in the experiment. By varying the R-space parameters and fitting the simulated V-space distributions to the data, the initial R-space distribution (for all three body coordinates) was deduced. These coordinates are, the O-H bond lengths (r_a and r_b) and the $\hat{HOH}$ angle (θ_r). The interactions between the different fragments resulting from the dissociation of a single molecule were treated as pair-wise screened Coulomb potentials (see Appendix A). Aside from structural parameters, the only adjustable quantity in the simulation that affects the angular distribution is the foil thickness. This value was measured in two independent ways: First by measuring the final charge state distributions produced after passing 4.5 MeV atomic O^+ ions through the target,[18] and second by comparing the experimental and simulated distribution of the sums of CM momenta for all fragments in a given event. Because the conservative Coulomb forces do not contribute to the momentum sums, these distributions represent the contributions of the nonconservative statistical processes to the fragment momenta. These distributions are structure independent but are strongly dependent upon target thickness. From both of these methods, the target thickness was found to be 100 ± 10 Å.

IV. RESULTS AND DISCUSSION

In this study we concentrated mainly on obtaining the density distribution describing only the bending mode of H_2O^+. The problem of determining the bond length distributions at such a low beam energy is slightly more complicated due to the necessity of incorporating electronic screening and will be discussed elsewhere.[19] Figure 1 shows the V-space angular distributions (θ_v) for three different final charge states of the oxygen fragment. These distributions have been measured simultaneously and therefore, excluding the final charge states, all of the experimental parameters are the same. The difference in the number of events in each of these histograms is representative of the charge state distribution of the outgoing oxygen ions. The

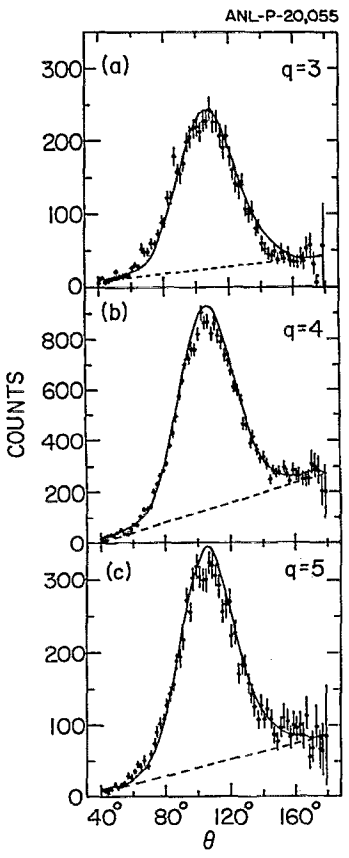

FIG. 1. V-space angular distributions (θ_v) for different final charge states (q) of the oxygen fragment: (a) $q=3$, (b) $q=4$, (c) $q=5$. The points with error bars correspond to the experimental results. The full line is the result of the simulation of 3000 trajectories (and then normalized to the data) using $\theta_e = 108.4°$. The broken line represents the fitted background.

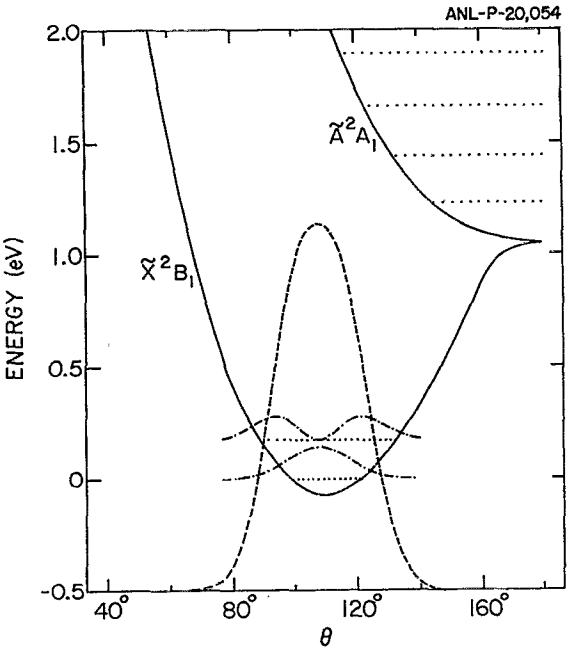

FIG. 2. Potential curves for H_2O^+ from Ref. 20. The dotted horizontal lines represent the different vibrational states. The chained curves represent the squares of the harmonic wave functions for the first two vibrational states. The dashed line is their superposition using the weights described in the text.

distributions are characterized by a peak above an apparent background. The backgrounds were approximated using a linear fit and are shown by dashed lines in Fig. 1. This background might be due to contributions from the $\tilde{A}^2A_1$ excited state[20] which is about 1 eV above the ionic ground state (see Fig. 2). Since the electron energy was well above the threshold, some population of the excited electronic state could contribute. For $q=4$, which is the most abundant charge state, the most probable angle, at which the distribution peaks is $[\theta_v]_{mp} = 106.6 \pm 0.2°$.

In order to deduce the most probable values for the R-space parameters (θ_r and the bond lengths), as well as the bending frequency ν_2, we simulated the experiment using a three-dimensional parametrized distribution in R-space. Since the probability distribution is the ensemble average of the square of the nuclear wave function, we use the form

$$P(r_a,r_b,\theta_r) = \mathscr{S}_1(r_1)\mathscr{S}_3(r_3)\mathscr{Q}(\theta_r), \tag{1}$$

where

$$r_1 = (r_a + r_b)/2, \tag{2}$$

$$r_3 = (r_a - r_b)/2. \tag{3}$$

In the harmonic approximation, the symmetric and antisymmetric bond length distributions are given by

$$\mathscr{S}_1 = \exp[-(r_1 - r_c)^2/\sigma_1^2], \tag{4}$$

$$\mathscr{S}_3 = \exp[-r_3^2/\sigma_3^2], \tag{5}$$

where in this approximation, r_c corresponds to the potential minimum r_e. The widths of each distribution are then given by

$$\sigma_1 = \sqrt{\hbar/2\pi\mu_1\nu_1}, \tag{6}$$

$$\sigma_3 = \sqrt{\hbar/2\pi\mu_3\nu_3}, \tag{7}$$

where $\mu_1 = 0.97$ amu and $\mu_3 = 0.93$ amu are the reduced masses for the symmetric and antisymmetric stretching modes, respectively. The frequencies ν_1 and ν_3 were chosen to be equal to 3213 and 3259 cm^{-1}, respectively (see Table I). It is important to point out that the exact value of those stretching frequencies has no influence on the the angular distribution. The angular distribution is then given by

$$\mathscr{Q}(\theta_r) = \sum_n f_n N_n \exp(-\xi^2) H_n^2(\xi), \tag{8}$$

where $H_n(\xi)$ is the Hermite polynomial of order n, N_n are normalization constants, f_n are the vibrational population factors, and

$$\xi = (\theta_r - \theta_c)/\sigma_2, \tag{9}$$

where θ_c corresponds to the minimum of the potential (θ_e in the harmonic approximation). The value of σ_2 is given by

$$\sigma_2 = \sqrt{\hbar/2\pi\mu_2\nu_2}, \tag{10}$$

where $\mu_2 = 0.43$ amu·Å^2 is a reduced mass defined so that the bending kinetic energy is given by $1/2\mu_2\dot{\theta}^2$. The sum

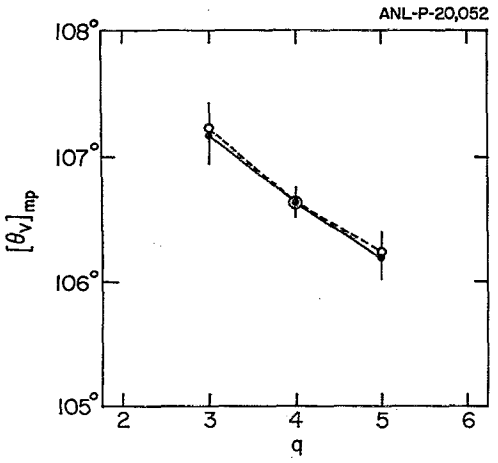

FIG. 3. Most probable value of the V-space angle $[\theta_v]_{mp}$ as a function of the charge state of the oxygen. The closed and open circles are the experimental and the simulated results, respectively. The R-space value used in the simulation was $\theta_c \simeq \theta_e = 108.4°$.

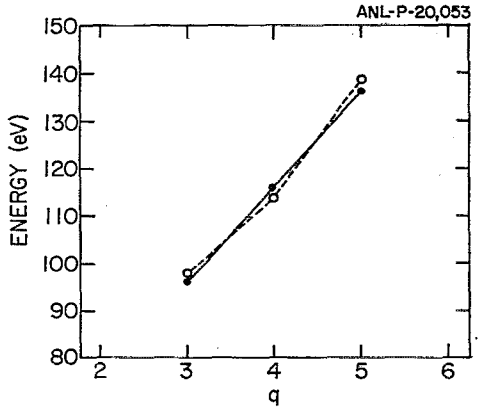

FIG. 4. Most probable value of the kinetic energy distribution of the protons as a function of the charge of the oxygen. The closed and open circles are the experimental and the simulated results, respectively. The bond length used in the simulation was $r_e = 1.00$ Å.

in Eq. (8) is needed in order to take account of the vibrational state population produced by electron impact ionization of H_2O. At room temperature, the excited state population of the parent neutral is negligible, and therefore for the f_n we used the Franck–Condon (FC) factors which have been previously measured.[1,21] We set the values of f_n in Eq. (8) to $f_0 = 0.85$, $f_1 = 0.15$, and $f_n = 0$ for $n > 1$ as measured by Diebeler.[21] Figure 2 shows the bending potentials for the ground and first electronic excited states of H_2O^+ as given by Jungen *et al.*[20] Also shown are the R-space distributions [the individual terms of Eq. (8)] for the lowest two vibrational states of the ground electronic state. The dashed line represents the initial distribution $\mathcal{Q}(\theta_r)$ taking account of the FC weighting of these two levels. The value of θ_c, r_c, and ν_2 were varied until the best fit to the data was obtained for the most probable charge state ($q = +4$). Using these values, simulations were carried out for the other charge states. For comparison with the data, the simulated distributions were added to the measured backgrounds and these results can be seen in Fig. 1 as solid lines. The values of the three parameters for which the best fit was obtained are shown in Table I, and agree with the previous spectroscopic measurements.

Another feature of these V-space distributions, which can be seen in Fig. 3, is a shift of the peak toward lower angles for higher charge states. This can be understood by the fact that for higher charge states, the oxygen ions recoil more than for lower charge states, while the proton–proton interaction is independent of the charge states, and this tends to close the angle in V-space. This is naturally accounted for in the simulations, as shown in Fig. 3, where the closed symbols are the experimental results and the open symbols are the simulated results. Correspondingly, the charge-state-dependence of the measured kinetic energy distributions is shown in Fig. 4. This is also accounted for by the simulation as shown in the same figure by the open circles.

The value of θ_c at which the best fit is obtained is $\theta_c = 108.4° \pm 0.5°$ which is in good agreement with the theoretical values of θ_e listed in Table I, as well as the value inferred spectroscopically by Dinelli *et al.*[8] The value of θ_c that we extract is the most direct measurement of θ_e reported so far.

V. CONCLUSIONS

The angular distribution of H_2O^+ has been measured using the CEI technique and the values of θ_e, ν_2, and r_e have been extracted from the data with relatively high precision for the angle. The results agree with previous experimental and theoretical values for this well-studied molecule. This provides an important quantitative test of the CEI method.

It is clear by now that the CEI method can be used to get relatively high precision values for some structural parameters. Although we needed to assume previously measured Franck–Condon factors to fit the full extent of the angular distribution in this experiment, this is not an inherent limitation of the method. A source of cold molecular ions will enable us to measure the ground state geometries of polyatomic molecular ions. Such an ion source is currently under development in our laboratory.

ACKNOWLEDGMENT

This work was supported by the U.S. Department of Energy, Office of Basic Energy Sciences, under Contract No. W-31-109-ENG-38.

APPENDIX

The screened potential between each pair of fragments inside the solid was given by

$$V(r) = (q_1 q_2 / r) e^{-r/\alpha_i}, \tag{A1}$$

where r is the distance between the two fragments, q_1 and q_2 are the charges and the exponential term reflects the

screening due to target electrons. The screening constant α_i is proportional to the beam velocity and given[22] by $\alpha_i = v/\omega_p$ where ω_p is the plasma frequency of the solid. At our velocity, α_i is very long ($\alpha_i = 4.5$ Å) compared to internuclear distances and thus has negligible influence on the results.

Outside the target, the potential between each proton and the oxygen was assumed to have the form

$$V(r) = \frac{(Z_1 - 2)Z_2}{r} e^{-r/\alpha_0} + \frac{q_1 q_2}{r}(1 - e^{-r/\alpha_0}), \quad \text{(A2)}$$

where Z_1 and Z_2 are the nuclear charge of the oxygen and the proton, respectively. The screening constant α_0 is of the order of the oxygen L-shell radius. Using hydrogenic wave functions, we calculated this radius and get the value $R_L = \alpha_0 = 0.4$ Å. For this value of α_0, the simulation gives an excellent fit to the final velocities as seen by the charge-state dependence of the final kinetic energies (see Fig. 4). The uncertainty in the value of α_0 is the principal contribution to the error in the measured bond length quoted in Table I.

[1] C. R. Brundle and D. W. Turner, Proc. R. Soc. London Ser. A **307**, 27 (1968).
[2] A. W. Potts and W. C. Price, Proc. R. Soc. London Ser. A **326**, 181 (1972).
[3] R. N. Dixon, G. Duxbury, J. W. Rabalais, and L. Åsbrink, Mol. Phys. **31**, 423 (1976).
[4] H. Lew and I. Heiber, J. Chem. Phys. **58**, 1246 (1973).
[5] H. Lew, Canadian J. Phys. **54**, 2028 (1976).
[6] G. Herzberg and H. Lew, Astronom. Astrophys. **31**, 123 (1974).
[7] P. A. Wehinger, S. Wyckoff, G. H. Herbig, G. Herzberg, and H. Lew, Astrophys. J. **190**, L46 (1974).
[8] B. M. Dinelli, M. W. Crofton, and T. Oka, J. Mol. Spectrosc. **127**, 1 (1988).
[9] S. E. Strahan, R. P. Mueller, and R. J. Saykally, J. Chem. Phys. **85**, 1252 (1986).
[10] J. A. Smith, P. Jørgensen, and Y. Öhrn, J. Chem. Phys. **62**, 1285 (1975).
[11] P. J. Fortune, B. J. Rosenberg, and A. C. Wahl, J. Chem. Phys. **65**, 2201 (1976).
[12] A. D. Esposti, D. G. Lister, P. Palmieri, and C. D. Esposti, J. Chem. Phys. **87**, 6772 (1987).
[13] Z. Vager, R. Naaman, and E. P. Kanter, Science **244**, 426 (1989).
[14] A. Faibis, W. Koenig, E. P. Kanter, and Z. Vager, Nucl. Instrum. Methods B **13**, 673 (1986).
[15] A. Belkacem, A. Faibis, E. P. Kanter, W. Koenig, R. E. Mitchell, Z. Vager, and B. J. Zabransky, Rev. Sci. Instrum. **61**, 946 (1990).
[16] D. S. Gemmell and Z. Vager, in *Treatise on Heavy-Ion Science*, edited by D. A. Bromley (Plenum, New York, 1985), Vol. 6, p. 243.
[17] D. Zajfman, G. Both, E. P. Kanter, and Z. Vager, Phys. Rev. A **41**, 2482 (1990).
[18] G. Both, E. P. Kanter, Z. Vager, B. J. Zabransky, and D. Zajfman, Rev. Sci. Instrum. **58**, 424 (1987).
[19] O. Heber, D. Kella, R. Naaman, Z. Vager, and D. Zajfman, to be published.
[20] CH. Jungen, K-E. J. Hallin, and A. J. Merer, Molec. Phys. **40**, 25 (1980).
[21] W. H. Dibeler, J. A. Walker, and H. M. Rosenstock, J. Res. Nat. Bur. Stand. A **70**, 459 (1966).
[22] J. D. Jackson, *Classical Electrodynamics* (Wiley, New York, 1975), 2nd ed.